140. Conformational Flexibility of the Acetoxyphenyl Group Studied by Statistical Analysis of Crystal Structure Data

by **Wolfgang Hummel**[a]), **Aleksander Roszak**[b]), and **Hans-Beat Bürgi**[a])*

[a]) Laboratorium für chemische und mineralogische Kristallographie, Universität Bern, Freiestr. 3, CH–3012 Bern

[b]) Institute of Chemistry, N.Copernicus University, Gagarina 7, PL–87-100 Toruń

(26.V.88)

The preferred conformation of the acetoxyphenyl fragment shows a planar acetoxy (AcO) group perpendicular to the Ph ring. Steric hindrance strongly limits and affects rotation about the C–$OCOCH_3$ bond: if the AcO group twists away from its perpendicular conformation, the carbonyl oxygen moves to keep the nonbonded distance to the atoms in *ortho*-position maximal. This is achieved by some twisting about the O–$COCH_3$ bond correlated with angle bending at the *ipso*-C-atom and ester O-atom. The maximum observed deviation away from the perpendicular conformation is ~ 47°. In the case of one or two *ortho*-hydrogens, deviations of the AcO group from the perpendicular conformation tend to be larger than in the case of two substituents.

Introduction. – Syntheses and measurements of optical properties (*e.g.* luminescence and laser emission) of 9-acetoxy-10-phenylanthracene derivatives have been described [1] [2]. Their laser activity depends to some extent on the position and conformation of an additional acetoxy substituent (AcO) on the Ph group [1]. Recently, accurate crystal structure determinations were done on some of these compounds [3]. Results of a study of the geometry and conformational flexibility of the acetoxyphenyl group in various environments are now reported.

Selection and Organization of the Data. – Crystal structures containing acetoxyphenyl (AcOPh) groups were retrieved from the *Cambridge Structural Database* (*CSD*, version of Sept. 1985 with 47165 entries in the bibliographic file) with programs provided by the *Cambridge Crystallographic Data Centre* [4]. The structural fragment shown in *Fig. 1* was searched for with the *CSD* connectivity search program CONNSER. No

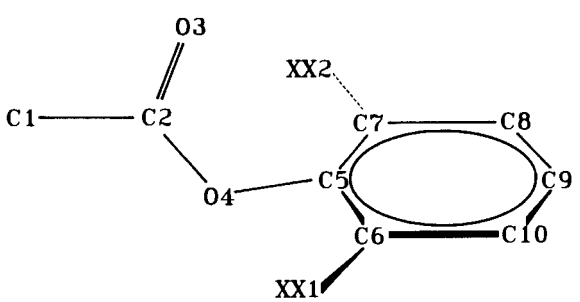

Fig. 1. *Atom types and numbering scheme in the AcOPh fragment.* XX1 and XX2 imply any type of non-metallic substituents.

restrictions were placed on the nature of the substituents at C(6) to C(10). Atomic coordinates of 75 structures were retrieved and calculations of geometric parameters performed with the program GEOM78. Names were assigned to geometrical parameters as follows: Dxy are bond lengths (*e.g.* bond C(1)–C(2) is D12), Axyz are bond angles, and Txyzw are torsion angles. Twist deformations about the bonds C(2)–O(4) and O(4)–C(5) are defined as in [5]:

$$\tau_{(C(2)-O(4))} = (T1245 + T3245 + 180)/2 \text{ [deg]}$$

$$\tau_{(O(4)-C(5))} = (T2456 + T2457 + 180)/2 \text{ [deg]}$$

Out of plane deformations at C(2) and C(5) are defined as in [5]:

$$\chi_{(C(2))} = (T1245 - T3245 - 180)/2 \text{ [deg]}$$

$$\chi_{(C(5))} = (T2456 - T2457 - 180)/2 \text{ [deg]}$$

The following test ranges were included in the geometry calculations: 1.40 Å $\leq$ D12 $\leq$ 1.60 Å, 1.10 Å $\leq$ D23 $\leq$ 1.28 Å, 1.28 Å $\leq$ D24 $\leq$ 1.40 Å, 1.30 Å $\leq$ D56, D57 $\leq$ 1.50 Å, and 115° $\leq$ A657 $\leq$ 130°. This avoids matching the search fragment with substructures of the same connectivity between non-H-atoms but different degrees of unsaturation [6]. Entries with $R > 0.12$ or $\sigma(C-C)_{av} > 0.03$ Å and structures with error flags or with partial disorder of the AcO group were rejected. The resulting list from GEOM78 was inspected by hand to remove structures containing transition metal atoms as well as data referring to lactones in structures with multiple phenolate ester fragments. The final list contains 102 AcOPh fragments in 56 structures. A list of reference codes [4] is available from the authors.

For each molecule, four symmetry-related isometric conformations exist as shown in *Fig. 2* (two if XX1 and XX2 are unequal). The symmetry operations interconverting the

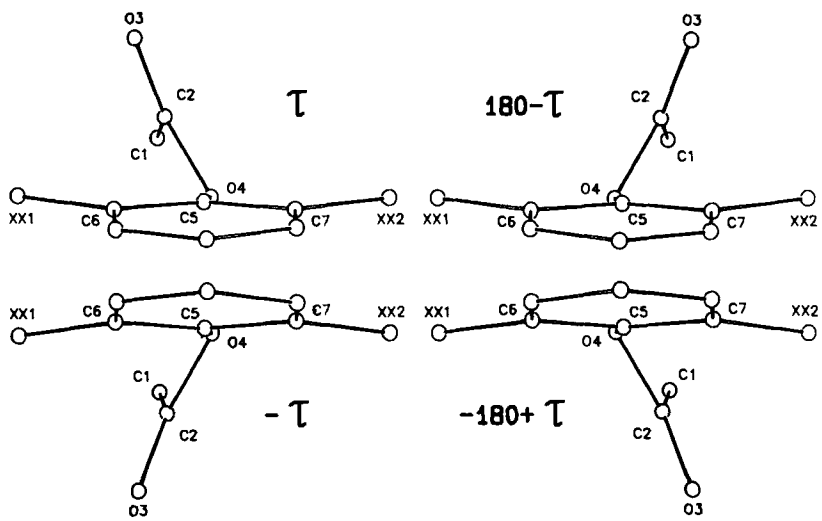

Fig. 2. *Symmetry-related conformations of the non-rigid AcOPh fragment.* The labels τ, $-\tau$, $180 - \tau$, and $-180 + \tau$ show their relationship in terms of the twist angle $\tau_{(O(4)-C(5))}$ (see text).

conformations may be taken to a first approximation as internal rotations of the mirror-symmetric AcO group with respect to the Ph group showing *mm*2 symmetry (*m* symmetry, if XX1 ≠ XX2) [7]. Conformational space may, thus, be partitioned into four asymmetric units with $0° \leq \tau_{(O(4)-C(5))} < 90°$, $90° \leq \tau_{(O(4)-C(5))} < 180°$, $-90° \leq \tau_{(O(4)-C(5))} < 0°$, and $-180° \leq \tau_{(O(4)-C(5))} < -90°$. A fragment as taken from the database will be found randomly in one of the four asymmetric units, and before doing any statistical analysis, all the fragments have to be transformed into the same asymmetric unit. To choose the latter as $0° \leq \tau_{(O(4)-C(5))} < 90°$, the following tests and transformations are necessary:

1) If T2456 < 0°, then change the signs of all torsional angles. This corresponds to transformations from $-\tau$ to τ and from $-180 + \tau$ to $180 - \tau$ *(Fig. 2)*.

2) If T1245 < 0°, then add 360° to T1245. T1245 is now in the range of 0° to 360° instead of −180° to +180°.

3) If $\tau_{(O(4)-C(5))} > 90°$, then exchange D56 with D57 and A456 with A457, $\tau_{(O(4)-C(5))new} = 180° - \tau_{(O(4)-C(5))}$, $\tau_{(C(2)-O(4))new} = 360° - \tau_{(C(2)-O(4))}$, and $\chi_{(C(2))new} = -\chi_{(C(2))}$ (not needed, if XX1 ≠ XX2).

Standard deviations of mean values (σ_m) are related to standard deviations of populations (σ_p, given in *Table 1*) by $\sigma_m = \sigma_p/\sqrt{N}$ where N is the number of data used for calculating means.

Discussion. – *Mean Geometry.* For calculating the mean geometry of the fragment the symmetry and shape of the data distribution has to be taken into account [8]. The distribution in *Fig. 3*, for example, consists of two asymmetric units (0° ≤ τ < 90° and 90° ≤ τ < 180°). It is symmetric about τ = 90°. The same distribution is also found between

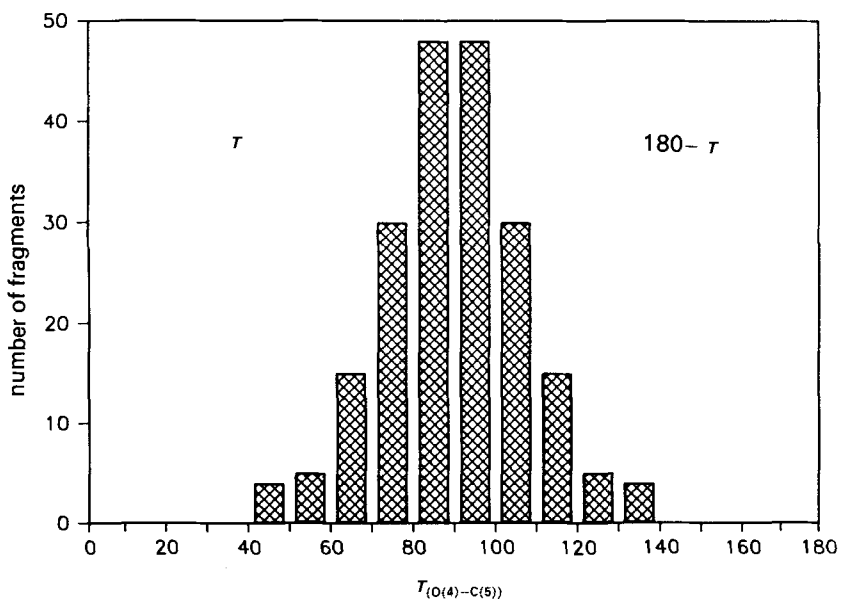

Fig. 3. *Histogram of* $\tau_{(O(4)-C(5))}$ *twist angles in AcOPh fragments.* τ and 180 − τ correspond to the symmetry related conformations in *Fig. 2*. Here, XX1 and XX2 are considered equivalent, even if they are chemically different.

Table 1. *Averaged Bond Lengths* [Å], *Bond Angles* [°], *and Torsion Angles* [°] (standard deviations of populations (σ_p) in parentheses)

	N[a])	⟨D12⟩	⟨D23⟩	⟨D24⟩	⟨D45⟩	⟨D56⟩	⟨D57⟩	
XX1 ≠ H ≠ XX2	70*	1.494(21)	1.194(20)	1.363(15)	1.402(19)	1.387(19)	1.387(19)	
XX1 = H ≠ XX2	47	1.490(21)	1.188(11)	1.358(18)	1.403(12)	1.376(15)	1.388(19)	
XX1 = H = XX2	40*	1.490(19)	1.181(15)	1.346(20)	1.411(12)	1.372(16)	1.372(16)	
All cases together	204*	1.491(21)	1.188(16)	1.357(18)	1.404(15)	1.382(19)	1.382(19)	
Anthracene deriv.[b])	32*	1.490(8)	1.189(8)	1.356(11)	1.406(9)	1.384(9)	1.384(9)	
Aryl esters[c])	11	1.497(16)	1.191(5)	1.352(20)	1.402(13)	–	–	
Acyclic esters[c])	118	1.495(19)	1.195(7)	1.340(14)	1.447(15)	–	–	
	N[a])	⟨A123⟩	⟨A124⟩	⟨A324⟩	⟨A245⟩	⟨A456⟩	⟨A457⟩	⟨A657⟩
XX1 ≠ H ≠ XX2	70*	127.1(1.2)	111.1(1.4)	121.8(1.5)	117.9(1.3)	118.9(1.9)	118.9(1.9)	122.1(1.8)
XX1 = H ≠ XX2	47	127.3(1.7)	110.6(1.5)	122.1(1.6)	118.1(1.8)	118.5(1.9)	119.1(1.7)	122.3(1.3)
XX1 = H = XX2	40*	126.4(1.4)	111.1(1.3)	122.4(0.9)	118.5(1.2)	118.8(1.5)	118.8(1.5)	122.2(0.9)
All cases together	204*	127.0(1.5)	110.8(1.4)	122.1(1.4)	118.1(1.6)	118.8(1.8)	118.8(1.8)	122.2(1.4)
Anthracene deriv.[b])	32*	127.0(0.6)	110.5(0.8)	122.5(0.6)	117.6(1.3)	118.6(1.6)	118.6(1.6)	122.7(0.9)
Aryl esters[c])	11	126.7(1.6)	110.6(0.8)	122.7(1.1)	118.9(1.7)	–	–	–
Acyclic esters[c])	118	125.4(1.2)	111.2(1.0)	123.4(0.9)	117.4(1.6)	–	–	–
	N[a])	$\langle\chi_{(C(2))}\rangle$	$\langle\chi_{(C(5))}\rangle$	$\langle\tau_{(C(2)-O(4))}\rangle$	$\langle\tau_{(O(4)-C(5))}\rangle$	$\tau_{(O(4)-C(5))}$min	$\tau_{(O(4)-C(5))}$max	
XX1 ≠ H ≠ XX2	70*	0.0(1.2)	1.9(1.1)	180.0(6.7)	90.0(12.7)	57.3	122.7	
XX1 = H ≠ XX2	47	–0.4(1.1)	2.1(1.1)	179.4(4.9)	85.6(18.5)	45.3	114.9	
XX1 = H = XX2	40*	0.0(1.4)	2.2(0.6)	180.0(3.9)	90.0(19.9)	42.7	137.3	
All cases together	204*	0.0(1.3)	2.1(1.0)	180.0(5.4)	90.0(17.3)	42.7	137.3	
Anthracene deriv.[b])	32*	0.0(0.7)	1.9(0.7)	180.0(6.0)	90.0(19.9)	54.1	125.9	

[a]) The asterisk indicates that due to symmetry the number of unique data is $N/2$.

[b]) Taken from [3].

[c]) Taken from [9].

$-180° \leq \tau < 0°$. Thus, the total distribution is bimodal with one maximum at $\tau = 90°$ and another at $\tau = -90°$. The mean geometry with respect to two asymmetric units, for which $0° \leq \tau < 180°$, is given in *Table 1*. Mean values calculated from a small set of very accurate data ($\sigma(C-C)_{av} < 0.005$ Å) on aryl esters [9] *(Table 1)* differ by less than $2\sigma_m$ from the present results, which also agree with results based on the 9-acetoxy-10-phenyl-anthracenes analysis [3] *(Table 1)*; the largest difference is about $2\sigma_m$.

On average the AcOPh group is planar ($\tau_{(C(2)-O(4))} = 180°, \chi_{(C(2))} = 0°$) and perpendicular to the Ph ring ($\tau_{(O(4)-C(5))} = 90°$). Atom O(4) lies out of the Ph plane by about 0.09 Å ($\chi_{(C(5))} = 2.1°$, *Fig. 4*: empty circles). O(3) and O(4) are on opposite sides of the plane.

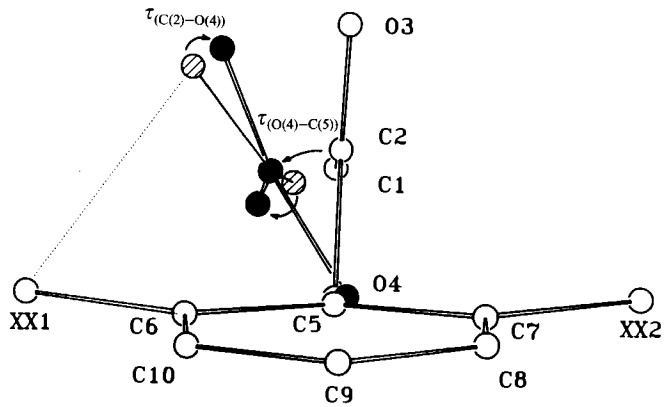

Fig. 4. *Superposition of AcOPh fragments showing the conformational flexibility of the AcO group.* Empty circles and black circles are real structures, dashed circles show a hypothetical case with $\tau_{(O(4)-C(5))} \neq 90°$ and $\tau_{(C(2)-O(4))} = 180°$ (see text).

As seen in *Table 1*, the average geometry of the AcO group is close to that derived for acyclic esters [9]. The only exception is the O(4)–C(5) bond which is about 0.04 Å longer, when the C-atom belongs to an alkyl group instead of a Ph ring ($C(sp^3)$ *vs.* $C(sp^2)$). As noted by *Schweizer* and *Dunitz* [9], the C(2)=O(3) carbonyl bond length in an ester seems to be relatively short; here it is 1.19 Å, 0.03 to 0.04 Å shorter than in amides [10].

The average C–C–C angle ⟨A657⟩ is significantly greater than 120° indicating the σ-electron withdrawing character of the AcO group in accordance with the general distortion pattern of substituted Ph rings [3b] [11].

Conformational Flexibility. As can be seen in *Fig. 3* and *Table 1*, the twist angle $\tau_{(O(4)-C(5))}$ shows a large standard deviation. A smaller but still significant standard deviation was found for $\tau_{(C(2)-O(4))}$. Two dimensional scatterplots of various combinations of torsion angles and bond angles showed some correlations. Thus, factor analysis [12] was employed to find relevant multidimensional correlations. The main results of this analysis are given in *Table 2*. The first two principal components account for 95% of the total variance and are statistically significant for a conservative estimate of the average experimental error in angles ($\sim 1.5°$ from $\sigma(C-C) = 0.03$ Å).

A pictorial interpretation of the first eigenvector (87% of total variance) is given in *Fig. 4* as a superposition of AcOPh fragments: If the AcO group twists away from its

Table 2. *Results of Principal Component Analysis of Bond Angles and Torsion Angles of the Acetoxyphenyl Group*

	All cases	XX1, XX2 = H	XX1 = H ≠ XX2	XX1, XX2 ≠ H
Observations	204[a])	40[a])	47	70[a])
Variables	11	11	11	11
Total variance	348.78	423.90	395.69	226.27
Principal component		Eigenvalue (% variance)		
1	87.39	94.10	89.88	77.20
2	7.64	3.05	6.03	14.17
3	1.14	0.80	1.35	2.50
4	1.11	0.74	1.06	2.09
5	0.77	0.46	0.70	1.45
6	0.75	0.32	0.44	0.90
7	0.56	0.29	0.26	0.75
8	0.41	0.17	0.17	0.60
9	0.21	0.07	0.11	0.34
10	0.00	0.00	0.00	0.00
11	0.00	0.00	0.00	0.00
Angles [°]		Eigenvector 1[b])		
A123	0.000	0.000	0.009	0.000
A124	0.000	0.000	–0.016	0.000
A324	0.000	0.000	0.005	0.000
A245	0.000	0.000	–0.066*	0.000
A456	–0.046*	–0.047*	–0.044*	–0.039*
A457	0.046*	0.047*	0.064*	0.039*
A657	0.000	0.000	–0.019	0.000
$\tau_{(C(2)-O(4))}$	–0.113*	–0.078*	–0.083*	–0.301*
$\tau_{(O(4)-C(5))}$	0.991*	0.995*	0.991*	0.952*
$\chi_{(C(2))}$	0.002	–0.018	0.002	0.013
$\chi_{(C(5))}$	0.000	0.000	–0.014	0.000
Angles [°]		Eigenvector 2[b])		
A123	0.000	0.000	0.037	0.000
A124	0.000	0.000	–0.061	0.000
A324	0.000	0.000	0.013	0.000
A245	0.000	0.000	–0.142	0.000
A456	–0.093	–0.028	–0.193	–0.091
A457	0.093	0.028	0.123	0.091
A657	0.000	0.000	–0.070	0.000
$\tau_{(C(2)-O(4))}$	0.986*	0.994*	0.955*	0.948*
$\tau_{(O(4)-C(5))}$	0.103	0.074	0.054	0.292*
$\chi_{(C(2))}$	–0.025	–0.072	–0.049	0.004
$\chi_{(C(5))}$	0.000	0.000	–0.004	0.000

[a]) Due to symmetry, the number of unique data equals one half of the number given.
[b]) The asterisk indicates significant components of eigenvectors.

preferred perpendicular conformation towards the Ph plane (*Fig. 4*: empty circles →dashed circles), the decrease in the nonbonded distance from O(3) to XX1 (*Fig. 4*: dotted line) is partially compensated by two accompanying distortions: *1)* Twisting of O(3) and C(1) around the axis C(2)–O(4) (*Fig. 4*: dashed circles →filled circles); *2)* bending the entire AcO group away from XX1 by increasing the angle O(4)–C(5)–C(6) (A456). The AcO group itself remains planar.

Table 2 shows results of a principal component analysis on the covariance matrix. The effects described above are expressed quantitatively in terms of the components of the first eigenvector *(Table 2, Column 1)* : an increase of $\tau_{(O(4)-C(5))}$ by 10° is correlated with a decrease of $\tau_{(C(2)-O(4))}$ by −1.1° and a decrease of A456 by −0.5° (and, by symmetry an increase of A457 by +0.5°). The effect on $\chi_{(C(2))}$ is vanishing small. Changes in the other parameters are zero due to symmetry.

The second eigenvector (7.6% of total variance) reflects most of the remaining variance of $\tau_{(C(2)-O(4))}$. This is seen most clearly in a scatterplot of $\tau_{(O(4)-C(5))}$ *vs.* $\tau_{(C(2)-O(4))}$ for the special case of two non-H *ortho*-substituents discussed below *(Fig. 5)*. The

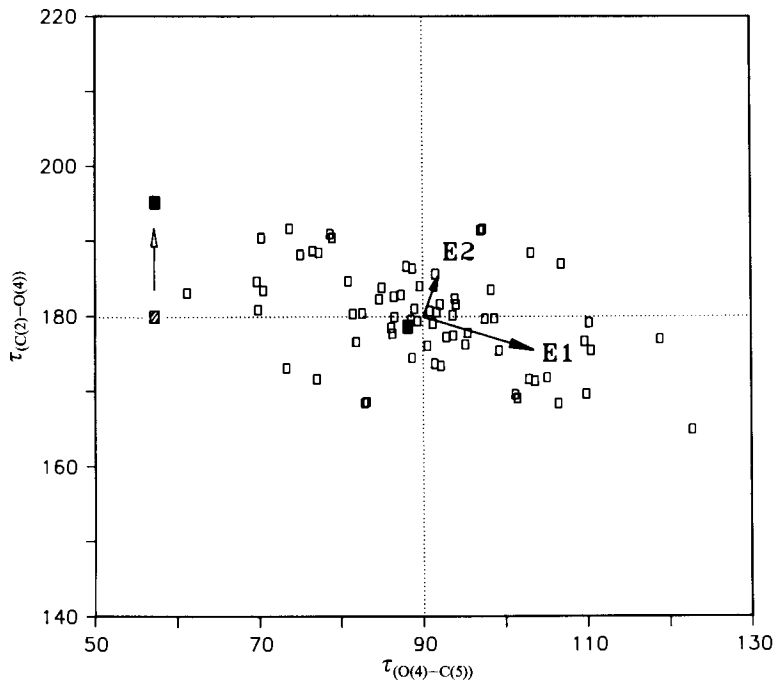

Fig. 5. *Scatterplot of twist angles* $\tau_{(C(2)-O(4))}$ vs. $\tau_{(O(4)-C(5))}$ *for the case of two non-H* ortho-*substituents.* E1 and E2 are projections of eigenvectors 1 and 2, respectively (see *Table 2*). Filled squares correspond to the superimposed structures shown in *Fig. 4*. The dashed square corresponds to the hypothetical dashed structure in *Fig. 4*. The intersection of the dotted lines indicate the mean geometry of the fragment.

projections E1 and E2 of the first two eigenvectors onto the $\tau_{(O(4)-C(5))}$–$\tau_{(C(2)-O(4))}$ plane are drawn as arrows from the center of the distribution. In order to show their relative importance, their lengths are chosen as the square roots of the variance explained by each vector. E1 is parallel to the long axis of the ellipsoidal distribution describing the correlation of $\tau_{(O(4)-C(5))}$ and $\tau_{(C(2)-O(4))}$. E2 is almost perpendicular to E1 and, thus, very close to the short axis of the distribution which accounts for data scatter independent of E1. The second eigenvector indicates that the correlation between $\tau_{(C(2)-O(4))}$ and $\tau_{(O(4)-C(5))}$ is not very strict. In energetic terms, one might state that a deformation of fixed magnitude is less costly along E1 than along E2.

Influence of ortho-*Substituents.* To study the influence of *ortho*-substituents on the geometry and conformational flexibility of the AcO group, the data set of 102 fragments was divided into three subsets: XX1 = XX2 = H (20 fragments), XX1 = H ≠ XX2 (47 fragments), XX1, XX2 ≠ H (35 fragments).

Mean geometries and factor analyses were calculated for each group separately *(Tables 1* and *2)*. The results reveal a consistent picture of the influence of non-H *ortho*-substituents on the conformational flexibility:

1) *Mean Geometries.* The distribution of $\tau_{(O(4)-C(5))}$ is slightly shifted in the case of one non-H *ortho*-substituent with a maximum around 85°. As expected, the preferred conformation is an AcO group pointing away from the non-H substituent XX2.

The variance of $\tau_{(O(4)-C(5))}$ increases with the number of *ortho*-hydrogens, whereas the variance of $\tau_{(C(2)-O(4))}$ decreases. In the case of two non-H substituents the minimum twisting angle $\tau_{(O(4)-C(5))}$ observed is 57.3°. But even when XX1 = XX2 = H, the coplanar conformation seems very unfavorable; the lowest twist angle observed is 42.7°.

It is tempting to correlate the small but systematic decrease in the mean distances D23 and D24 with the increase in $\sigma[\tau_{(O(4)-C(5))}]$. One might argue that the conformational flexibility increases with decreasing size of the substituents XX1, XX2, and that this affects not only the width of the distribution of $\tau_{(O(4)-C(5))}$ but also enlarges the mean square amplitudes of internal libration of the $OCOCH_3$ group about the O(4)–C(5) bond. As a consequence, the distances D23 and D24 would appear to be shorter for XX1 = H = XX2 than for XX1, XX2 ≠ H [13].

Another small but systematic influence of *ortho*-substituents concerns the C–C bond lengths D56 and D57: in the case of non-H substituents, the mean distances are more than 0.01 Å longer (D57 for XX1 = H ≠ XX2) than in the case of H substituents. The means and variances of the other parameters do not seem to be affected by the nature of *ortho*-substituents.

2) *Correlations.* For two non-H substituents, the steric coupling between $\tau_{(C(2)-O(4))}$ and $\tau_{(O(4)-C(5))}$ is seen most clearly *(Fig. 5)*; an increase of $\tau_{(O(4)-C(5))}$ by 10° is correlated with a decrease of $\tau_{(C(2)-O(4))}$ by −3.2°, an effect that is about four times larger than in the other two subsets *(Table 2)*.

Another effect becomes apparent too: as the twist angle $\tau_{(O(4)-C(5))}$ decreases the AcO group bends away from the Ph group by opening the angle A245. For XX1 = H = XX2 the available data at low $\tau_{(O(4)-C(5))}$ are somewhat meager but the pattern is clear *(Fig. 6a)*. It is most pronounced in the case of XX1 = H ≠ XX2 *(Fig. 6b)*.

In summary there are two ways of minimizing nonbonded strain in conformations deviating from $\tau_{(O(4)-C(5))} = 90°$: *1)* if XX1 ≠ H the main effect is twisting about $\tau_{(C(2)-O(4))}$. *2)* If XX1 = H, the angle A245 opens up, whereas the twist deformation $\tau_{(C(2)-O(4))}$ is relatively small.

A final remark about a general lesson to be learned from the present study: multivariate analysis of structural data for the AcOPh fragment has revealed a general picture of conformational flexibility that could not have been obtained by considering structures individually. In the first step of the analysis, an overall pattern of conformational flexibility was extracted from the data using a very general definition of the fragment. In the next step, *ortho*-H and non-H substituents were distinguished. This revealed different ways to release strain and showed that their relative importance varies with the nature of

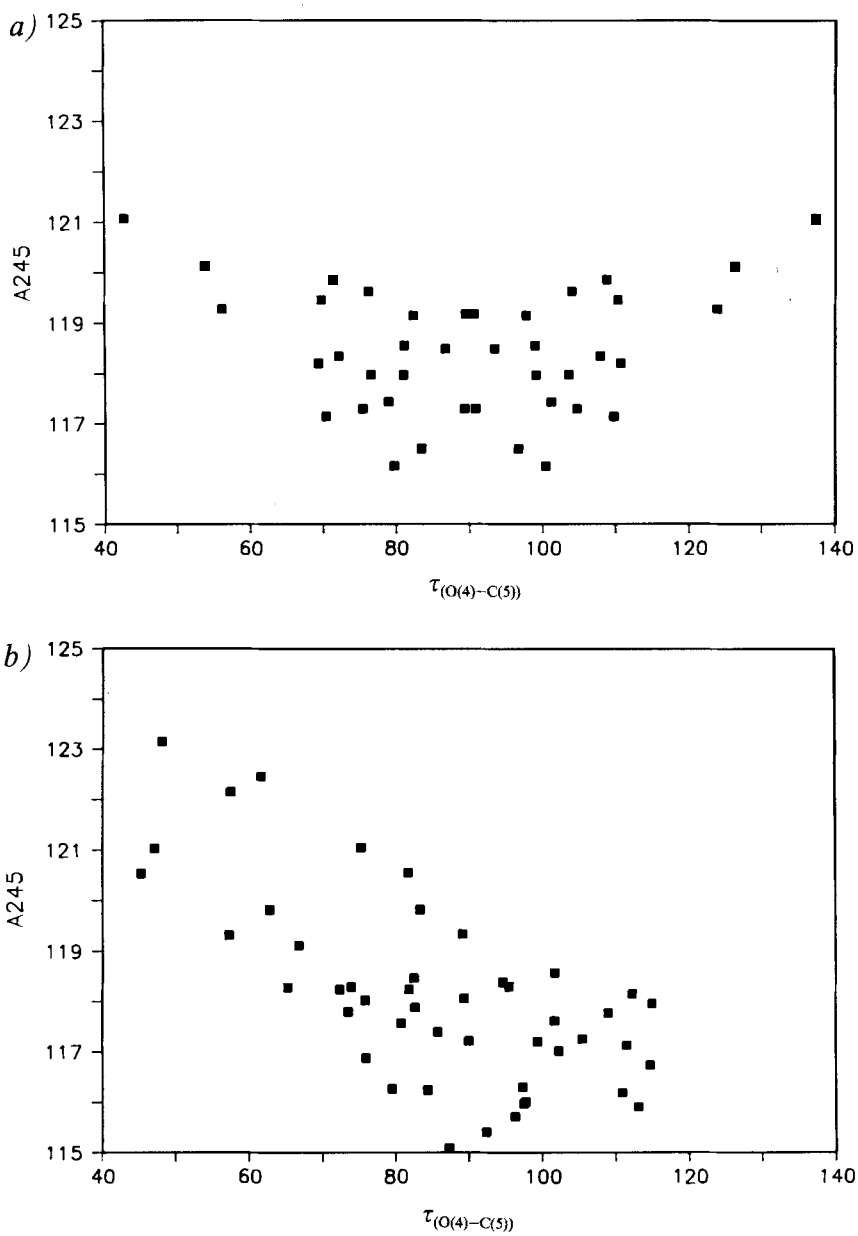

Fig. 6. a) *Scatterplot of bond angle C(2)–O(4)–C(5)* vs. $\tau_{(O(4)-C(5))}$ *for the case XX1 = H = XX2,* b) *scatterplot of bond angle C(2)–O(4)–C(5)* vs. $\tau_{(O(4)-C(5))}$ *for the case XX1 = H ≠ XX2*

ortho-substituents. A finer classification on the fragment type might give even more detailed information on the mechanisms of strain release but would imply fewer fragments per class and, therefore, statistically less significant results with respect to the fragment chosen.

REFERENCES

[1] J. R. Heldt, *Z. Naturforsch., A* **1983,** *38,* 1197.
[2] J. Gronowska, A. Dzielendziak, J. Heldt, *Acta Phys. Chem.* **1983,** *29,* 145, and ref. cit. therein.
[3] a) A. Roszak, Z. Skrzat, *Acta Crystallogr., Sect. C* **1985,** *41,* 1483; b) A. Roszak, T. Borowiak, *ibid.* **1986,** *42,* 343; c) A. Roszak, W. L. Duax, *ibid.* **1987,** *43,* 251; d) A. Roszak, T. Borowiak, *ibid.* **1987,** *43,* 498.
[4] F. H. Allen, S. Bellard, M. D. Brice, B. A. Cartwright, A. Doubleday, H. Higgs, T. Hummelink, B. G. Hummelink-Peters, O. Kennard, W. D. S. Motherwell, J. R. Rodgers, D. G. Watson, *Acta Crystallogr., Sect. B* **1979,** *35,* 2331.
[5] H. B. Bürgi, E. Shefter, *Tetrahedron* **1975,** *31,* 2976.
[6] P. Murray-Rust, J. Raftery, *J. Mol. Graph.* **1985,** 3, 60.
[7] H. C. Longuet-Higgins, *Mol. Phys.* **1963,** *6,* 445.
[8] P. Murray-Rust, *Acta Crystallogr., Sect. B* **1982,** *38,* 2765.
[9] W. B. Schweizer, J. D. Dunitz, *Helv. Chim. Acta* **1982,** *65,* 1547.
[10] P. Chakrabarti, J. D. Dunitz, *Helv. Chim. Acta* **1982,** *65,* 1555.
[11] A. Domenicano, P. Murray-Rust, *Tetrahedron Lett.* **1979,** *24,* 2283.
[12] SAS Institute Inc., 'SAS User's Guide: Statistics', 5th edn., Cary, NC: SAS Institute Inc., 1985, 621pp.
[13] J. D. Dunitz, V. Schomaker, K. N. Trueblood, *J. Phys. Chem.* **1988,** *92,* 856.